FOSSIL ENERGY

NIPER-326
(DE89000711)

SIMULATION OF PRODUCTION FROM WELLS WITH HORIZONTAL/SLANTED LATERALS

Final Report

By
Ming-Ming Chang

March 1989

Performed Under Cooperative Agreement No. FC22-83FE60149

IIT Research Institute
National Institute for Petroleum and Energy Research
Bartlesville, Oklahoma

Bartlesville Project Office
U. S. DEPARTMENT OF ENERGY
Bartlesville, Oklahoma

DISCLAIMER

Printed in the United States of America. Available from:
National Technical Information Service
U.S. Department of Commerce
5285 Port Royal Road
Springfield, VA 22161

NTIS price codes
Paper copy: **A03**
Microfiche copy: **A01**

NIPER-326
Distribution Category UC-122

SIMULATION OF PRODUCTION FROM WELLS WITH HORIZONTAL/SLANTED LATERALS

Final Report

By
Ming-Ming Chang

March 1989

Work Performed Under Cooperative Agreement No. FC22-83FE60149

Prepared for
U.S. Department of Energy
Assistant Secretary for Fossil Energy

Thomas B. Reid, Project Manager
Bartlesville Project Office
P.O. Box 1398
Bartlesville, OK 74005

Prepared by
IIT Research Institute
National Institute for Petroleum and Energy Research
P.O. Box 2128
Bartlesville, OK 74005

TABLE OF CONTENTS

TABLES

TABLES - Continued

ILLUSTRATIONS

ILLUSTRATIONS - Continued

SIMULATION OF PRODUCTION FROM WELLS WITH HORIZONTAL/SLANTED LATERALS

By Ming-Ming Chang

ABSTRACT

A horizontal and slanted well model was developed and incorporated into BOAST, a black oil simulator, to predict the potential production rates for such wells. The slanted/horizontal well model can be used to calculate the productivity index, based on the length and location of the wellbore within the block, for each reservoir grid block penetrated by the slanted/horizontal wellbore. The well model can be run under either pressures or rate constraints in which wellbore pressures can be calculated as an option of infinite-conductivity. The model is easy to use and can simulate the performance of multiple horizontal/slanted wells in any geometric combination within reservoirs.

The model was checked against the analytical formulas of transient wellbore pressure in an infinite slab reservoir. A close match having an average deviation of only ±4% was found between the analytical formula and the fully penetrating slanted well model after a production period of early radial flow. A good agreement was also obtained between the simulation results of the horizontal well model and published analytical curves. This is the first published mathematical model that has been validated for slanted well simulation.

Production rates from vertical wells, horizontal wells, and slanted wells of variable well lengths in a field of 40-acre well spacing were compared. During the pressure-depletion phase, about the same improvements in production rates over those of vertical wells were observed for horizontal and slanted wells which extended the same length from the plan view. The effects of eccentricity on horizontal well performance were examined. The effects of vertical permeability on the production rates of horizontal and slanted wells were also studied. As expected the vertical discontinuity of reservoirs showed insignificant effects on the production from slanted wells.

A field simulation of a horizontal well and its three offset conventional vertical wells demonstrated the application of the developed well model.

ACKNOWLEDGMENTS

The author acknowledges the financial support of this work by the Department of Energy through cooperative agreement DE-FC22-83FE60149 managed by the Bartlesville Project Office and TQR Inc. Thanks are also due to Min K. Tham of NIPER for his supervision, and Thomas Reid, Ephraim Ubani of the DOE Bartlesville Project Office, S. D. (Sada) Joshi of Phillips Petroleum Co. (currently with Joshi Production Technologies, Inc.) and Liviu Tomutsa and Nicida Maerefat of NIPER for their discussions and suggestions.

INTRODUCTION

The technology for drilling horizontal wells to increase reservoir drainage areas has been used for many years.[1] As the directional drilling technology has advanced, the cost of drilling directional wells has been reduced, and the accuracy of drilling has been significantly improved. Some 30 or more horizontal wells are presently successfully producing oil.

When compared with vertical drilling, directional drilling of laterals into a formation has a great potential for increasing the rate of production and ultimate recovery. It has been suggested that drilling of laterals can be competitive with hydraulic fracturing in stimulating production; however, horizontal laterals, especially slanted laterals, are expensive to drill, and the increase in production over that from vertical wells is difficult to predict. In planning these operations,the increase in the drainage area from the use of horizontal and slanted laterals should be predicted, and the effect of potential sweep efficiencies of any future enhanced oil recovery projects should be established. The literature contains reports[2-7] on some attempts to calculate productivity from horizontal wells; however, all of these tools are analytical equations which can be applied only to homogeneous media under steady-state conditions.

Conventional vertical wells are drilled perpendicular to and horizontal wells parallel to the upper and lower formation bounding planes. Most vertical wells do not penetrate the formation as planned; instead, there is a certain angle between the well axis and the normal to the formation plane. These types of slanted wells, because of their long wellbores, could provide similar enhancement in productivity but more tolerance to the vertical discontinuity of reservoirs than horizontal wells. In spite of their

potential advantages, slanted wells have received only limited interest compared to that of horizontal wells. Attempts have been made to compare horizontal and slant well productivities in reservoirs with different thicknesses.[2]

Because of restrictions to applying existing analytical formulas in evaluating the performance of horizontal/slanted wells, there is a need to modify a black oil simulator to simulate horizontal and slanted well production.

LITERATURE SURVEY

About 120 horizontal wells were drilled in the midcontinent region in the 1930's,[1] and since then others were drilled in Alaska,[8] New Mexico,[9] Canada,[10] France, and offshore Italy.[11]

During the 1950's, electrical models[2,12-13] were used in the laboratory to study the production performance of horizontal wells. Diagrams for estimating increases in the productivity of horizontal wells versus that of vertical wells were presented. These studies concentrated on the improvement of the productivity index (PID) of horizontal wells over that of vertical wells. Because of the limitations of the physical model used in those studies, only a few properties such as wellbore length and formation thickness were examined.

Merkulov[14] presented the first analytical equation found in the literature for calculating the productivity of horizontal wells. Recently, a few other investigators derived similar analytical formulas. Giger[4] reported criteria, in addition to the productivity formula, for choosing horizontal rather than vertical wells, and in another paper[15] he analyzed the advantages of horizontal wells for producing from reservoirs having heterogeneities such as fractures and permeability variations. Based on the analytical formula developed by Giger, Karcher[3] further studied the productivity of horizontal wells having coning problems. Joshi[2] derived a PID equation different from that of Giger.[4] All of the above mathematical analyses for horizontal well productivity predictions were based on the assumption of steady state. They provided an estimation of productivity or injectivity for horizontal wells when the pressure drop between the formation and the wellbore stays constant, such as with the waterflooding process.

In contrast to the steady-state assumption in the PID formula, the pressure transient behavior for horizontal wells in finite and infinite reservoirs was studied by other investigators.[5-7] These well testing analyses assumed single-phase flow in slab reservoirs with finite pay zone thicknesses. Goode and Thambynayagam[6] reported the pressure response of horizontal wellbores in semi-infinite reservoirs in which one of the areal extents is bounded. Clonts and Ramey[7] and Ozkan et al.[5] developed type curves for well testing horizontal wells in infinite reservoirs. Daviau et al.[16] reported a similar analysis to calculate the transient pressure of horizontal wells in both infinite and semi-infinite reservoirs. All of the developed solutions indicate an initial radial flow in the vertical plane with the drainage radius equal to one-half of the payzone thickness. This is followed by a pseudoradial or a pseudosteady state flow for infinite and semi-infinite reservoirs, respectively.

For the same reason as that of horizontal wells, slanted wells increase well productivity by increasing the producing-interval area exposed to flow. Roemershauser[17] studied steady-state flow in a reservoir producing through a fully penetrating slanted well using an electrical model. Roemershauser considered a circular reservoir of finite extent and concluded that the slant of a fully penetrating well causes an increase in well productivity. Cinco[18] presented the first mathematical analysis of pressure transient response for slanted wells. Type curves were reported at five dimensionless formation thicknesses and five slanted angles ranging from 15° to 75°. Cinco proposed an equation to calculate skin factor resulting from slanted angles, and Van Der Vlis[19] later proposed an equation to calculate the effective wellbore radius of a slanted well. The calculations of productivities of slanted wells using the equations of Cinco and Van Der Vlis were found to be in excellent agreement.

In addition to their potential for increasing primary production, horizontal/ slanted wells have been suggested for enhanced oil recovery (EOR) applications to increase injectivity and sweep efficiency. Rial[20] found from his steamflooding simulation that the heat transmissibility was higher throughout the grid system using the horizontal well model than the conventional vertical well. The temperature and oil phase saturation distribution revealed an improved sweep efficiency and, therefore, a higher

oil recovery with a horizontal wellbore. Huang's simulation study[21] indicated that horizontal wells can be effective for reducing or preventing steam override in the steamflooding process. In addition to the thermal application, a study of horizontal wells used in miscible or CO_2 flooding was recently conducted by Chen.[22] He used a simulation model to quantify the increase in CO_2 sweep efficiency that results from using horizontal wells and found that the greatest percentage increase in areal sweep efficiency occurred at conditions that provided the most adverse mobility ratio. Chen suggested the use of "tilted" horizontal wells in situations where reservoirs are layered, with poor communication between the layers. Instead of running a simulation test using a "tilted" well model, Chen estimated the improvement in sweep efficiency of tilted wells from simulation results of horizontal wellbores located in different layers. Butler[23] derived a formula to estimate the drainage rate of heavy oil around an expanding steam chamber which is above a horizontal well. Butler then compared his theoretical prediction to scaled experiments in the laboratory. Another physical model study of horizontal wells was conducted on the sweep efficiency of CO_2 flooding. Jones[24] found, from his laboratory investigation, an increase in oil production of 24% when horizontal wells were used for CO_2 injection as compared to the use of vertical injection wells.

The numerical simulation study conducted on horizontal/slanted wells was focused on the production performance of such wells. Relatively less work was done on the representation of this horizontal/slanted well model within the numerical simulator. Lee[25] studied the productivity of inclined or slanted wells using a boundary integral method. By comparing numerical solutions derived by the boundary integral method, Lee concluded that the commonly used well productivity formula[26,27] for the finite difference method could yield erroneous results for slanted wells. Williamson and Chappelear[28,29] presented a comprehensive discussion on the installation of a well model in a numerical simulator, including problems which may be encountered and possible remedies.

DESCRIPTION OF BOAST AND ITS WELL MODEL

The black oil applied simulation tool (BOAST) has become popular for reservoir engineering studies by both industry and academia since it was released by the Department of Energy in 1982. BOAST is a three-dimensional,

three-phase (oil, water, and gas) black oil simulator based on continuity equations and Darcy's expression as a momentum balance for each phase. BOAST is designed for the simulation of primary depletion, pressure maintenance by water and/or gas injection, and basic secondary recovery operations such as waterflooding in a black oil reservoir.

BOAST assumes that fluid and rock properties are single-valued functions of pressure only. No mass transfer between different phases is allowed. The finite-difference matrix representing the fluid flow within reservoir grid blocks is solved implicitly for pressure. The saturation is then solved explicitly. This numerical technique used to solve pressure differential equations is called the implicit pressure-explicit saturation (IMPES) method. The boundary conditions include no flow boundary of the reservoir and source/sink incorporated through the well model.

BOAST uses the IMPES numerical procedure which has both advantages and limitations. The IMPES method requires less computing time and smaller storage space than the fully implicit method. But IMPES is not as stable as the fully implicit method when small grid sizes or very high flow rates, which result in rapid changes in saturation, are used. In such cases, the computer time step must be reduced significantly to maintain the numerical stability.

As with other reservoir simulators, BOAST uses an analytical well model to represent flow within a grid block where it enters or leaves a well. According to the boundary conditions chosen by users, two types of well model are available: pressure constraint and rate constraint. When pressure constraint is used, wellbore pressures must be assigned, and well rates are calculated by coupling the reservoir and wellbore flows through a local, approximate, steady, singular solution of radial flow equations. When rate constraint is applied, wellbore pressure is back calculated from the same local, radial flow equations.

The production/injection well is treated as sink/source in BOAST. The productivity index (PID) concept is used in the sink/source model to couple reservoir and wellbore flows as follows:

$$Q_o = PID\ (k_{ro}/\mu_o B_o)\ (P_e - P_{wf}) \qquad (1)$$

where Q_o is the oil rate, k_{ro} is the oil relative permeability, μ_o is the oil viscosity, B_o is the oil formation volume factor, P_e is the wellbore block pressure, and P_{wf} is the wellbore pressure.

Only conventional vertical well models are considered in BOAST. Productivity index for each vertical wellbore block is calculated as follows:

$$PID = \frac{0.00708\ (k_x\ k_y)^{\frac{1}{2}} h}{\ln \frac{r_o}{r_w} + s} \tag{2}$$

where k_x, k_y are permeability (md) in x and y directions, respectively.
h is the thickness (ft) of wellbore block,
r_w is the wellbore radius (ft),
r_o is the equivalent radius (ft) of wellbore block,
s is the skin factor.

Peaceman[26] derived an analytical formula for calculating r_o in nonsquare grid blocks with anisotropic permeability as follows:

$$r_o = 0.28 \frac{[(k_y/k_x)^{\frac{1}{2}} \Delta x^2 + (k_x/k_y)^{\frac{1}{2}} \Delta y^2]^{\frac{1}{2}}}{(k_y/k_x)^{\frac{1}{4}} + (k_x/k_y)^{\frac{1}{4}}} \tag{3}$$

where Δx, Δy are lengths (ft) of wellbore block in x and y directions, respectively.

For a square grid block with isotropic permeability in the horizontal direction, formula 3 can be reduced to:[27]

$$r_o = 0.2\ \Delta x \tag{4}$$

WELL MODEL DEVELOPMENT

Slanted/Horizontal Well Model

A slanted/horizontal well model was developed to calculate the productivity index for each reservoir grid block penetrated by a slanted/horizontal wellbore. Figure 1 shows the flow chart of this slanted/horizontal well subroutine.

Based on the location of the horizontal (or vertical/slant) well defined in the reservoir grids, the well model first determines reservoir grid blocks penetrated by the wellbore. It then calculates the PID for the wellbore within each penetrated grid block. The PID value of each wellbore block is computed from the wellbore length and geometric location of the wellbore within the block. Since the wellbore may not be parallel to the boundaries of its rectangular reservoir block, the slanted/horizontal wellbore located anywhere in a rectangular block was first broken down into three vector components in x, y, and z directions as shown in figure 2. The productivity index of the wellbore block was then calculated separately for the three components (PID_x, PID_y, PID_z), assuming that the well was located in the middle of the wellbore contained in the rectangular block. The calculated productivity indexes in x, y, and z directions were combined later as the productivity index of the slanted/horizontal wellbore for that block, as:

$$\vec{PID} = \vec{PID}_x + \vec{PID}_y + \vec{PID}_z \tag{5}$$

An analytical well model developed by Abou-Kassem and Aziz[30] is used for computing the PID value for the wellbore component located anywhere in a rectangular block. This analytical model was derived from the concept of image wells (fig. 3). This analytical formula calculates the equivalent wellbore radius (r_o), a key value in computing PID as:

$$r_o = \left(\exp\left(-2\pi f\right) \prod_i \left[r_i^{T_i} i_{,1} \prod_j \left(\frac{r_{ij}}{a_j}\right)^{T_i}\right]\right)^b \tag{6}$$

where a_j = distance from well (j = 1) to its jth image, ft

$$b = 1/\sum_i T_i \tag{7}$$

f = fraction of well associated with the well block

γ_{ij} = distance from grid point i to well j (i = 1...8; j = 1...9), ft; well (j = 1) is located in grid 0

T_i = transmissibility coefficient for flow from block i to the well block

The developed slanted/horizontal well model can be used to calculate the wellbore productivity for both nonboundary and boundary blocks which contain up to four reservoir boundaries. The wellbore productivity index could decrease drastically when the wellbore is located near the reservoir boundary.

The slanted/horizontal well in this model was defined in either of the following two ways: (1) input the starting and ending grid blocks of the slanted wellbore or (2) input the starting grid block, the well length, the slant angel, and the angle away from the x-direction from the plan view. The wellbore does not have to be parallel or perpendicular to the boundaries of reservoir grid blocks. The wellbore can be inclined from the horizontal or vertical direction. Simply stated, the wellbore can be assigned in any geometric location within the reservoir. In addition, this well model can describe a combination of multiple wells of any geometric combination of vertical/horizontal/slanted wellbore or any number of drainholes (fig. 4).

Modification of Existing Well Models

The existing subroutine "QRATE"[31] was modified to compute the well rate and/or wellbore pressure for both slanted/horizontal and vertical wells. Similar to the treatment to the vertical well model within BOAST, this slanted/horizontal well model can be run under either rate or pressure constraints. Under the constraint of the constant production/injection rate, the wellbore pressure is back calculated from the assigned flow rate. The pressure constraint in the slanted/horizontal well model is treated in two ways: explicit pressure or implicit pressure. The flow rate under the explicit pressure constraint is calculated for each grid block containing the slanted/horizontal wellbore, based on its mobility ratio and formation volume factor. Under the implicit pressure constraint, the pressure matrix derived from the diffusivity equations is modified before being solved. The well rate

is then calculated using the modified subroutine "PRATEO."

Infinite Conductivity Option

The approach to simulate the well performance above (or in the original BOAST simulator), under the rate constraint, is closed to the "uniform-flux" condition, in which the wellbore rates in different wellbore blocks are about the same and the wellbore pressure could be different from block to block because most drainholes are drilled and cased. An infinite-conductivity drain hole is closer to reality than a uniform-flux wellbore; therefore, a new option of infinite-conductivity was added into the slanted/horizontal well model. The infinite-conductivity condition translates mathematically into a uniform-pressure (or uniform potential) condition at the well. This means that the flux at different points of the well is determined in such a way that the potential is uniform through the wellbore. To calculate these fluxes within wellbore blocks, two conditions must be applied: fluxes must sum to the required total rate, and a uniform potential at the well results. Mathematically, these conditions can be expressed as follows:

(a) When the oil flow rate (q_o) is specified:

$$q_o = \sum_{i=1}^{n} q_{oi}$$

$$= \sum_{i=1}^{n} \left[\left(\frac{k_r}{B\mu} \right)_{oi} (PID)_i \ (P_i - P_{wf}) \right] \qquad (8)$$

where q_{oi} is the flow rate in the ith wellbore block;
k_r, B, μ, and PID are relative permeability, formation volume factor, viscosity, and productivity index, respectively;
n is the number of blocks containing horizontal wellbores; and
P_i, P_{wf} are the ith wellblock pressure and bottomhole pressures, respectively.

Since k_r, B, μ, and PID are known for each block, equation 8 can be rewritten as:

$$q_o = \sum_{i=1}^{n} D_i (P_i - P_{wf}) \qquad \text{where } D_i = \left(\frac{k_r}{B\mu}\right)_{oi} (PID)_i$$

$$= \sum_{i=1}^{n} D_i P_i - P_{wf} \sum_{i=1}^{n} D_i$$

$$P_{wf} = \frac{1}{\sum_{i=1}^{n} D_i} \left(\sum D_i P_i - q_o\right)$$

Once the bottomhole pressure is determined, the flow rate in each wellbore block can be calculated as:

$$q_{oi} = D_i \left(P_i - P_{wf}\right)$$

(b) When the total flow rate (q_t) is specified, a similar approach to it in (a) can be used:

$$q_t = q_{ot} + q_{wt} + q_{gt}$$

$$= \sum_{i=1}^{n} \left[\left(\frac{k_r}{B\mu}\right)_{oi} + \left(\frac{k_r}{B\mu}\right)_{wi} + \left(\frac{k_r}{B\mu}\right)_{gi}\right] (PID)_i (P_i - P_{wf})$$

$$= \sum_{i=1}^{n} C_i \left(P_i - P_{wf}\right)$$

$$= \sum_{i=1}^{n} (C_i P_i - C_i P_{wf})$$

where subscripts o, w, and g indicate oil, water, and gas phases, respectively;

and $C_i = \left[\left(\frac{k_r}{B\mu}\right)_{oi} + \left(\frac{k_r}{B\mu}\right)_{wi} + \left(\frac{k_r}{B\mu}\right)_{gi}\right](PID)_i$;

then

$$P_{wf} = \frac{1}{\sum_{i=1}^{n} C_i} \left(\sum_{i=1}^{n} C_i P_i - q_t\right)$$

and $$q_{oi} = \left(\frac{k_r}{B\mu}\right)_{oi} (PID)_i (P_i - P_{wf})$$

$$q_{wi} = \left(\frac{k_r}{B\mu}\right)_{wi} (PID)_i (P_i - P_{wf})$$

$$q_{gi} = \left(\frac{k_r}{B\mu}\right)_{gi} (PID)_i (P_i - P_{wf})$$

WELL MODEL VERIFICATION

Slanted Well Model

Cinco's analytical formula[18] was used as a benchmark to verify the slanted well model developed in this study. A close match having an average deviation of only ±4% was found between the analytical formula and the fully penetrating slanted well model after a production period of the early radial flow.

Three-dimensional (20x19x10) simulations were conducted in an infinite slab reservoir to simulate the transient wellbore pressure of a fully penetrating slanted well at various slant angles and formation thicknesses. The reservoir and well properties that comprised the numerical model are listed in table 1. Figure 5 shows the comparison of dimensionless pressure drawdown between simulation results of the slanted well model and analytical curves at five slanted angles ranging from 15° to 75°. Good agreements were found when dimensionless time was greater than 400 (or 30 seconds in this simulation study). The formation thickness for the simulation studies in figure 5 was 300 feet. Simulation results from this study are compared to the analytical solutions of slanted wells at these slant angles in tables 2 through 6.

Good agreements were also obtained. As shown in figure 6, the slant angle was 60° and the formation thickness ranged from 30 to 1,500 feet which corresponded to 100 to 5,000 in dimensionless thickness. Tables 6 through 10 show the comparisons of simulation results against the analytic solutions at 60° slant angle and various formation thicknessses.

The good agreements obtained above indicate that the slanted/horizontal well model developed in this study appears to be capable of predicting the production behavior of slanted wells.

Horizontal Well Model

The horizontal well model can be treated as a special case of the developed slanted well model when the angle is 90 degrees. The horizontal well version of the slanted/horizontal well model was successfully tested in two- and three-dimensional runs, with and without vertical wells. Different options including rate constraint, explicit pressure constraint, and implicit pressure constraint were also verified. Table 11 lists the well types, well constraints, and wellblock coordinates used in the four simulation tests of the horizontal well model.

To verify the numerical results of this horizontal well model, analytical formulas developed by others[5,6] were used as benchmark checks. The agreement of simulation results of our model and Ozkan et al's. analytical type curve[5] was good, as shown in figure 7. The simulated horizontal well is 2,000 ft long in the center of 50 ft of pay zone and an infinite reservoir. The remaining parameters assigned in the simulator, listed in table 12, were the same as those in the sample problem of Ozkan et al.[5]

The other analytical formula compared was the pressure drawdown of a horizontal well in a semi-infinite reservoir.[6] This 500-ft horizontal well is in the middle of a formation which is 220 ft in thickness, 2,100 ft in the x direction, and infinite length in the y direction. Table 13 lists the reservoir, fluid, and well properties used in the simulation model. Figure 8 shows the comparison between the simulation results obtained in this study and the analytical curve in example problem 1 of Goode et al.[6] A close match was obtained except during the first 0.2 hour and also the time period from 10 to 300 hours. The discrepancy at the early time period might have resulted from the numerical error associated with the gridding and/or the disregard of the gravity effect in developing the analytical formula. The disagreement during the flow time from 10 to 300 hours indicated that our simulation model is more sensitive to the reservoir boundary than the theoretical prediction. It was found through various simulations that the numerical results were sensitive to both the time step used and the size of grid blocks containing and near the horizontal wellbore.

The developed horizontal well model in the BOAST simulator appears to be capable of predicting the production behavior of horizontal wells after being compared with the published theoretical formula.

SIMULATION STUDIES OF PRODUCTION FROM HORIZONTAL AND SLANTED WELLS

The primary production rates from vertical wells, horizontal wells, and slanted wells of variable well lengths were compared for a field of 40 acres with 50 ft formation thickness. The reservoir properties are listed in table 14. Figure 9 shows one-half of the 3-dimensional (15x15x5) reservoir grid blocks used in the numerical study. The lengths of horizontal wells located in the center of the formation ranged from 100 to 1,350 ft, and the angles of slanted wells varied from 63° to 88°. A refined numerical grid block system (18x15x15) was used for simulation studies of horizontal wells at 50 ft and slanted wells at angles of 45°, 31° and 22°.

The horizontal wells or the slanted wells, as expected, showed faster recovery rates from a formation of low permeability than the vertical well because of the larger formation area exposed to the wellbore of the horizontal or slanted wells. Figure 10 shows the cumulative oil production over 5 years from a fully penetrating vertical well and horizontal wells with well lengths from 50 to 1,350 ft. The horizontal wells are assigned in the middle of the formation of 50 ft thickness. To evaluate the performance from the horizontal wellbore, only the productions from the horizontal sections -- not including the 25 ft of vertical penetration -- were studied. A homogenous formation permeability of 1 md in both horizontal and vertical directions was assumed in simulation runs. As shown in figure 10, the production was higher for those horizontal wells that had longer wellbores. As the production proceeded, the cumulative production of the long horizontal well started to level because of a faster pressure depletion of the reservoir fluid from the long horizontal wellbore. The 5 years of production from a 50-ft horizontal well was 6% more than that from a fully penetrating vertical well of the same wellbore length.

When the well length increased, the additional production enhancement from the increase of wellbore length decreased. Figure 11 shows a comparison of oil rates from different portions of horizontal wells to rates from a vertical well with 50 ft wellbore length. During the first 100 days of production, the increase of wellbore length contributed approximately the same amount of additional well productivity. As the production time proceeded, the contribution to the oil rate from the additional wellbore length became less important. After 5 years of production from this case, the production increase from the 1,350-ft wellbore over that of the 750-ft well was

insignificant. This is due to the effect of the limited size of the reservoir. Because the reservoir pressure is depleted after 5 years of primary production, longer wellbore can do little in enhancing the production.

A study of the effect of eccentricity on a horizontal well with 350 ft of wellbore was conducted. Figure 12 shows the comparison of 5 years of production from horizontal wells located at different distances from the top of the reservoir. The horizontal well located in the middle of the reservoir produced fastest among the five cases studied, followed by the wellbore immediately below the formation center and the one immediately above the formation center. The horizontal wellbore near the reservoir boundary produced less than the other three cases. Because of the gravity effect, the horizontal well near the bottom of the reservoir produced more than a horizontal well the same distance away from the top of the reservoir.

Figure 13 shows the production of slanted wells with angles from 22° to 88°. Similar to the results from horizontal wells, the slanted well which has a larger slant angle; therefore, a longer wellbore showed a higher cumulative production and an earlier reduction in well rate than one with less slant angle. Comparing figure 13 to figure 10, about the same improvements in production rates over those of vertical wells were observed between horizontal and slanted wells which extended the same length from the plan view. Table 15 listed this comparison of cumulative production between horizontal and slanted wells after 5 years. With a same well length of 100 ft from the plan view as that of a horizontal well, the slanted well (63° slant angle) had a wellbore length of 112 ft. Because of a longer wellbore, this 63° slanted well in 5 years produced 1.5% more than the horizontal well of 100 ft. As the horizontal wellbore became longer, the slanted well with the same length from the plan view had about the same wellbore length as the horizontal well, as shown in table 15. Because of the effect of eccentricity on the slanted well, the horizontal well produced more than the slanted well of the same well length from the plan view at slant angles over 76°. For an extreme case, in which horizontal/slanted wells penetrate the whole formation, such as the case of 1,350 ft wellbore in table 15, horizontal wells have about the same well length as slanted wells and the eccentricity effect is not so significant as in the short wellbore cases; therefore, horizontal wells show about the same cumulative production as slanted wells.

The effect of vertical permeability on the production of horizontal or slanted wells was studied. As shown in figures 14 and 15, the decrease of vertical permeability reduced the production from horizontal or slanted wells for all the cases studied. However, little effect from vertical permeability on the production from the vertical well was observed. The vertical permeability showed a more pronounced effect on horizontal wells (fig. 14) than on slanted wells (fig. 15). Since slanted wells are a combination of vertical and horizontal wells, slanted wells are affected less by vertical permeability than horizontal wells.

In addition to wellbore length (or slant angle for slanted wells), vertical permeability, and eccentricity effect, the advantage of horizontal or slanted wells over vertical wells also depends on the formation permeability. Figure 16 shows the following simulation study of permeability on reservoir production under different well geometries. For a 350-ft horizontal well located in the center of a reservoir of 40-acre well spacing with 50 ft formation thickness, the horizontal well produced 150% more than the vertical well during 5 years, at a formation permeability of 1 md. For a formation of 10 md permeability, the horizontal well produced about twice the amount of the vertical well after 250 days, but only 8% more than the vertical well after 5 years. When the permeability was increased to 100 md, the difference in cumulative production between the horizontal well and the vertical well was minimal after a production period of 3 months.

FIELD SIMULATION OF HORIZONTAL WELL PRODUCTION

Reservoir information and production data of oilfield A, in Eddy County, New Mexico, were collected for use in field simulation. The production of field A is from the Permian (Lower Leonard) Abo Reef dolomite at a depth of about 6,200 ft. The main producing mechanism is gravity drainage which is supplemented by the injection of the residual gas into the gas cap. Because of the high gas-oil ratio (GOR) produced from the volatile oil, the rapid depletion of reservoir pressure resulted in reduced ultimate oil recovery and gas coning which has become the most serious operating problem for field A. Producing from horizontal drainholes became the alternative to infill drilling.

Figure 17 shows the areal grid block of the part of field A studied in

this simulation. Horizontal well A was drilled in field A in 1979. The total length of the horizontal drainhole is 106 ft. Offset conventional wells B, C, and D were drilled and completed, ranging from 660 to 960 ft away, as shown in figure 17. Gas injection wells are north of well A, and water influx comes from the bottom aquifer on the south side and water injection wells on the east side. The oil production rates and produced GORs from 1979 to 1987 for wells A, B, C, and D were compiled for history match in simulation.

In a 15x15x5 three-dimensional simulation, the production histories of wells A, B, C, and D were matched. In addition to the above four oil production wells, one gas injection well in the top layer and one water injection well in the bottom layer were assigned in the reservoir model to simulate the gas/water injection in the formation. The relative permeabilities measured in cores from field A were used as the initial input. The PVT values (viscosity, formation volume factor, and amount of dissolved gas) with pressure were obtained from a PVT correlation package developed by Lewis Tech Service. The oil rates of four production wells were input into the simulation models, whereas gas saturations, pay zone thicknesses, and gas/water injection rates were adjusted to match the produced GOR for all four production wells. Figure 18 shows the match of GOR from 1979 to 1987 of the simulated horizontal well.

The history match of field A from the simulation study indicated that horizontal well A was near the bottom of the oil zone. Although the GOR of three offset conventional wells reached 10 Mcf/bbl after 2 years, the GOR of horizontal well A stayed at about 3 Mcf/bbl for 6 years. With a wellbore of only 106 ft, horizontal well A overproduced its offset conventional wells by locating its wellbore far away from the gas/oil contact area. After a history match by the simulation, the production of these four studied wells was evaluated using a GOR of 100 Mcf/bbl as the criterion to shut in. The simulation results showed that horizontal well A will produce more oil than the combination of its three offset conventional wells after January 1987.

CONCLUSIONS

Horizontal and slanted well models were developed in this study for the BOAST simulator to predict the potential production rates of fields. From the results of this study, the following conclusions were made:

1. Developed horizontal and slanted well models appear to be capable of predicting the production behavior for such wells. The comparisons of numerical models and analytical results of pressure transient tests for both horizontal and slanted wells showed good agreements.
2. In primary depletion production, about the same improvements in production rates over those of vertical wells were observed for horizontal and slanted wells which extended the same length from the plan view.
3. The advantage of horizontal/slanted wells over the vertical wells in production rates depends on the length of wellbore, slant angle, vertical permeability, eccentricity, and radial permeability.
4. Vertical permeability shows less effect on slanted wells than on horizontal wells in the production rate.

REFERENCES

1. Stormont, D. H. Increasing Drainage of Oil Into the Well by Drainage Drilling. Oil and Gas J., Aug. 17, 1953, pp. 105-108.

2. Joshi, S. D. Augmentation of Well Productivity Using Slant and Horizontal Wells. Pres. at the 61st SPE Tech. Conf. and Exhibition, New Orleans, LA, Oct. 1986. SPE Paper 15375.

3. Karcher, B. J., F. M. Giger, and J. Combe. Some Practical Formulas to Predict Horizontal Well Behavior. Pres. at the 61st SPE Tech. Conf. and Exhibition, New Orleans, LA, Oct. 1986. SPE Paper 15430.

4. Giger, F. M. The Reservoir Engineering Aspects of Horizontal Drilling. Pres. at the 59th SPE Tech. Conf. and Exhibition, Houston, TX, Sept. 1984. SPE Paper 13024.

5. Ozkan, E., R. Raghavan, and S. D. Joshi. Horizontal Well Pressure Analysis. Pres. at the SPE California Regional Meeting, May, 1987. SPE Paper 16378.

6. Goode, P. A., and R. K. M. Thambynayagam. Pressure Drawdown and Buildup Analysis of Horizontal Wells in Anisotropic Media. Pres. at the 60th SPE Annual Meeting, Las Vegas, NV, Sept., 1985. SPE Paper 14250.

7. Clonts, M. D. Pressure Transient Analysis for Wells With Horizontal Drainholes. Pres. at the 56th SPE Calif. Reg. Meeting., Apr. 1986. SPE Paper 15116.

8. Sherrard, D. W., B. W. Brice, and D. G. MacDonald. Application of Horizontal Wells at Prudhoe Bay. Pres. at the 61st SPE Tech. Conf. and Exhibition. New Orleans, LA, Oct. 1986. SPE Paper 15376.

9. Detmering, T. J. Update on Drainhole Drilling - Empire Abo. Proceedings of 31st Annual Southwestern Petroleum Short Course, Lubbock, TX, Apr. 1984, pp. 25-41.

10. MacDonald, R. R. Drilling the Cold Lake Horizontal Well Pilot No. 2. Pres. at the 60th SPE Tech. Conf. and Exhibition, Las Vegas, NV, Sept. 1985. SPE Paper 14428.

11. Reiss, L. H. Horizontal Wells' Production After Five Years. Pres. at the 60th SPE Tech. Conf. and Exhibition, Las Vegas, NV, Sept. 1985. SPE Paper 14338.

12. Landrum, B. L. Effect of Drainhole Drilling on Productivity Capacity. J. Pet. Tech., Feb. 1955, pp. 45-47.

13. Perrine, R. L. Well Productivity Increase from Drainhole as Measured by Model Studies. Petroleum Trans., AIME, v. 24, 1955, pp. 3034.

14. Merkulov, V. P. Le debit des puits devies et horizontaux. Neft. Khoz, v. 6, 1958, pp. 51-56.

15. Giger, F. M. Horizontal Wells Production Techniques in Heterogenous Reservoirs. Pres. at the SPE Middle East Meeting, Bahrain, March 1985. SPE Paper 13710.

16. Daviau, F., G. Mouronval, and G. Bourdarot. Pressure Analysis for Horizontal Wells. Pres. at the 60th SPE Tech. Conf. and Exhibition, Las Vegas, NV, Sept. 1985. SPE Paper 14251.

17. Roemershauser, A. E., and M. F. Hawkins, Jr. The Effect of Slant Hole, Drainhole, and Lateral Hole Drilling on Well Productivity. J. Pet. Tech., Feb. 1955, pp. 11-14.

18. Cinco, H., F. G. Miller and H. J. Ramey, Jr. Unsteady-State Pressure Distribution Created by a Directionally Drilled Well. J. Pet. Tech., Nov. 1975, pp. 1392-1400.

19. Van Der Vlis, A.C. Increasing Well Productivity in Tight Chalk Reservoir. Proceedings of the 10th World Petroleum Congress, v. 3, Bucharest, Hungary, 1979, pp. 71-78.

20. Rial, R. M. 3D Thermal Simulation Using a Horizontal Wellbore for Steam Flooding. Pres. at the 59th Tech. Conf. and Exhibition, Houston, TX, Sept. 16-19, 1984. SPE Paper 13076.

21. Huang, W. S. and M. A. Hight. Evaluation of Steamflood Pressures Using Horizontal Wells. Pres. at the SPE 1986 International Meeting, Beijing, China, Mar. 17-20. SPE Paper 14130.

22. Chen, S. M. and J. Olynyk. Sweep Efficiency Improvement Using Horizontal Wells or Tilted Horizontal Wells in Miscible Floods. Pres. at the 36th Annual Meeting of the Petroleum Society of CIM, Edmonton, Canada, June 2-5, 1985. CIM Paper 85-36-62.

23. Butler, R. M. and D. J. Stephens. The Gravity Drainage of Steam-Heated Heavy Oil to Parallel Horizontal Wells. Pres. at the 31st Annual Meeting of the Petroleum Society of CIM, Calgary, Alberta, May 25-28, 1980. Paper 80-31-31.

24. Jones, S. E. The Effect of Horizontal Wellbore Injection Versus Point-Source Injection on the Oil Recovery by CO_2. M. S. Thesis, Univ. of Wyoming, Laramie, WY 1986.

25. Lee, S. H. Analysis of Productivity of Inclined Wells and Its implication on Finite Difference Reservoir Simulation. Pres. at the 9th SPE Symposium on Reservoir Simulation, San Antonio, TX, Feb. 1-4, 1986. SPE Paper 16002.

26. Peaceman, D. W. Interpretation of Well-Block Pressures in Numerical Reservoir Simulation with Nonsquare Grid Blocks and Anisotropic Permeability. Soc. Pet. Eng. J., June 1983, pp. 531-43.

27. Peaceman, D. W. Interpretation of Well-Block Pressure in Numerical Reservoir Simulation. Soc. Pet. Eng. J., June 1978, pp. 183-94.

28. Williamson, A. S. and J. E. Chappelear. Representing Wells in Numerical Reservoir Simulation: Part 1 - Theory. Soc. Pet. Eng. J., June 1981, pp. 323-38.

29. Williamson, A. S. and J. E. Chappelear. Representing Wells in Numerical Reservoir Simulation: Part 2 - Implementation. Soc. Pet. Eng. J., June 1981, pp. 339-44.

30. Abou-Kassem, J. H. and K. Aziz. Analytical Well Models for Reservoir Simulation. Soc. Pet. Eng. J., Aug. 1985, pp. 573-579.

31. Fanchi, J. R., K. J. Harpole, and S. W. Bujnowski. BOAST: U. S. DOE Research Report DOE/BC/10033-3. U.S. Department of Energy, Bartlesville, OK, 1982.

TABLE 1. - Reservoir and well properties for pressure drawdown simulation of slanted wells

Porosity, %	10
Permeability, md	100
Thickness, ft	30 to 5,000
Oil formation volume factor, RB/STB	1.5
Rock compressibility, psi^{-1}	3×10^{-5}
Oil viscosity, cp	1.5
Flow rate, STB/day	1,500
Well radius, ft	0.3
Production time, days	10 to 374
Slant angles, degrees	15, 30, 45, 60, 75

TABLE 2. - Comparison of simulated pressure drawdown against analytical solution of slanted well (slant angle = 15° dimensionless thickness = 1,000).

Time		P_{wf}	ΔP[1]	P_d[2]	$(P_d)_a$[3]	Error (%) $\frac{\lvert P_d - (P_d)_a \rvert}{(P_d)_a} \times 100$
Day	t_d[4]					
$4x10^{-4}$	500	4975	55	3.46	3.39	2
$4x10^{-3}$	$5x10^{3}$	4962	68	4.28	4.50	5
0.04	$5x10^{4}$	4941	89	5.60	5.63	0.5
0.4	$5x10^{5}$	4921	109	6.86	5.76	1
4.0	$5x10^{6}$	4902	128	8.06	7.91	2

1. $\Delta P = (P_{ave})_i - P_{wf}$

   $(P_{ave})_i = 5030$ psi

2. $P_d = \frac{k_r h \Delta P}{(141.2)\, q_w \beta \mu} = \frac{(100)(300)\Delta P}{(141.2)(1500)(1.5)(1.5)} = 0.06295\ \Delta P$

3. From table 4, ref. 18.

4. t_d = dimensionless time = $\frac{(0.000264)\, K_r t\ (hr)}{\phi \mu\, C_t r_w^2}$

TABLE 3. - Comparison of simulated pressure drawdown against analytical solution of slanted well (slant angle = 30° dimensionless thickness = 1,000).

Time, day	t_d	P_{wf}	ΔP[1]	P_d[2]	$(P_d)_a$[3]	Error (%) $\frac{\lvert P_o - (P_d)_a \rvert}{(P_d)_a} \times 100$
$4x10^{-4}$	500	4982	48	3.02	3.04	~0
$4x10^{-3}$	$5x10^3$	4971	59	3.71	4.04	8
0.04	$5x10^4$	4953	77	4.85	5.07	4
0.4	$5x10^5$	4934	96	6.04	6.16	2
4.0	$5x10^6$	4915	115	7.24	7.29	0.7

1. $\Delta P = (P_{ave})_i - P_{wf}$

   $(P_{ave})_i = 5030$ psi

2. $P_d = \frac{k_r h \Delta P}{(141.2)\, q_w \beta \mu} = \frac{(100)\,(300)\,\Delta P}{(141.2)(1500)(1.5)(1.5)} = 0.06295 \Delta P$

3. From table 4 ref. 18.

TABLE 4. - Comparison of simulated pressure drawdown against analytical solution of slanted well (slant angle = 45° dimensionless thickness - 1,000).

Time, day	t_d	P_{wf}	ΔP[1]	P_d[2]	$(P_d)_a$[3]	Error (%) $\frac{\lvert P_d - (P_d)_a \rvert}{(P_d)_a} \times 100$
$4x10^{-4}$	500	4992	38	2.39	2.48	4
$4x10^{-3}$	$5x10^3$	4982	48	3.02	3.30	8
0.04	$5x10^4$	4967	63	3.97	4.18	5
0.4	$5x10^5$	4950	80	5.04	5.16	2
4.0	$5x10^6$	4932	98	6.21	6.27	2

1. $\Delta P = (P_{ave})_i - P_{wf}$

   $(P_{ave})_i = 5030$ psi

2. $P_d = \frac{k_r h\, \Delta P}{(141.2)\, q_w \beta \mu} = \frac{(100)(300)\Delta P}{(141.2)(1500)(1.5)(1.5)} = 0.06295\ \Delta P$

3. From table 4 ref. 18.

TABLE 5. - Comparison of simulated pressure drawdown against analytical solution of slanted well (slant angle = 75° dimensionless thickness - 1,000.)

Time		P_{wf}	ΔP[1]	P_d[2]	$(P_d)_a$[3]	Error (%) $\frac{\lvert P_d - (P_d)_a \rvert}{(P_d)_a} \times 100$
day	t_d					
$4x10^{-4}$	500	4985	45	0.85	2.91	7
$4x10^{-3}$	$5x10^{3}$	4971	59	1.12	1.21	7
0.04	$5x10^{4}$	4951	79	1.49	1.55	4
0.4	$5x10^{5}$	4925	105	1.98	2.05	3
4.0	$5x10^{6}$	4877	153	2.89	2.88	0

1. $\Delta P = (P_{ave})_i - P_{wf}$

   $(P_{ave})_i$ = 5030.4 psi

2. $P_d = \frac{k_r h \Delta P}{(141.2) q_w \beta \mu} = \frac{(100)(300)\Delta P}{(141.2)(5000)(1.5)(1.5)} = 0.0189\ \Delta P$

3. From table 4 ref. 18.

TABLE 6. - Comparison of simulated pressure drawdown against analytical solution of slanted well (slant angle = 60° dimensionless thickness = 1,000).

Time		P_{wf}	ΔP[1]	P_d[2]	$(P_d)_a$[3]	Error (%) $\frac{\lvert P_d - (P_d)_a \rvert}{(P_d)_a} \times 100$
day	t_d					
$4x10^{-4}$	500	5004	26.4	1.67	1.76	5
$4x10^{-3}$	$5x10^{-3}$	4996	34.4	2.17	2.33	7
0.04	$5x10^{4}$	4985	45.4	2.86	2.98	4
0.4	$5x10^{5}$	4971	59.4	3.74	3.78	1
40	$5x10^{6}$	4955	75.4	4.75	4.83	2

1. $\Delta P = (P_{ave})_i - P_{wf}$

   $(P_{ave})_i$ = 5030.4 psi

2. $P_d = 0.06295\ \Delta P$

3. From table 4 ref. 18.

TABLE 7. - Comparison of simulated pressure drawdown against analytical solution of slanted well (slant angle = 60° dimensionless thickness = 100).

Time		P_{wf}	ΔP[1]	P_d[2]	$(P_d)_a$[3]	Error (%) $\frac{\lvert P_d - (P_d)_a \rvert}{(P_d)_a} \times 100$
day	t_d					
4×10^{-5}	50	4797	199	1.25	1.18	6
4×10^{-4}	500	4750	246	1.55	1.83	15
4×10^{-3}	5×10^{3}	4612	384	2.42	2.63	8
0.04	5×10^{4}	4422	574	3.61	3.68	2
0.4	5×10^{5}	4221	775	4.88	4.82	1
4.0	5×10^{6}	4056	940	5.92	5.97	1

1. $\Delta P = (P_{ave})_i - P_{wf}$

   $(P_{ave})_i$ = 4996 psi

2. $P_d = \frac{k_r\, h\, \Delta P}{(141.2)\, q_w\, B\mu} = \frac{(100)(30)\,\Delta P}{(141.2)(1500)(1.5)(1.5)} = 0.006295\,\Delta P$

3. From table 1, ref. 18.

TABLE 8. - Comparison of simulated pressure drawdown against analytical solution of slanted well (slant angle = 60° dimensionless thickness - 200).

Time		P_{wf}	ΔP[1]	P_d[2]	$(P_d)_a$[3]	Error (%) $\frac{\lvert P_d - (P_d)_a \rvert}{(P_d)_a} \times 100$
day	t_d					
4×10^{-2}	500	4880	120	1.51	1.76	14
4×10^{-3}	5×10^{3}	4824	176	2.22	2.48	10
0.04	5×10^{4}	4748	252	3.17	3.37	6
0.4	5×10^{5}	4649	351	4.42	4.48	1
4.0	5×10^{6}	4555	445	5.60	5.62	1
10.9	138×10^{7}	4533	467	5.88	6.13	4

1. $\Delta P = (P_{ave})_i - P_{wf}$

   $(P_{ave})_i$ = 5000 psi

2. $P_d = \frac{k_r\, h\, \Delta P}{(141.2)\, q_w\, B\mu} = \frac{(100)(60)\Delta P}{(141.2)(1500)(1.5)(1.5)} = 0.01259\,\Delta P$

3. From table 2, ref 18.

TABLE 9. - Comparison of simulated pressure drawdown against analytical solution of slanted well (slant angle = 60° dimensionless thickness = 500).

Time, day	t_d	P_{wf}	ΔP[1]	P_d[2]	$(P_d)_a$[3]	Error (%) $\frac{\lvert P_d - (P_d)_a \rvert}{(P_d)_a} \times 100$
4×10^{-4}	500	4956	53	1.67	1.76	5
4×10^{-3}	5×10^{3}	4936	72	2.27	2.35	3
0.04	5×10^{4}	4911	98	3.09	3.10	0
0.4	5×10^{5}	4877	132	4.16	4.04	3
4.0	5.10^{6}	4837	172	5.42	5.16	5

1. $\Delta P = (P_{ave})_i - P_{wf}$

   $(P_{ave})_i$ = 5009 psi

2. $P_d = \frac{k_r h\, \Delta P}{(141.2)\, q_w \beta\mu} = \frac{(100)(150)\Delta P}{(141.2)(1500)(1.5)(1.5)} = .0315\ \Delta P$

3. From table 3, ref. 18.

TABLE 10. - Comparison of simulated pressure drawdown against analytical solution of slanted well (slant angle = 60° dimensionless thickness = 5,000.

Time, day	t_d	P_{wf}	ΔP[1]	P_d[2]	$(P_d)_a$[3]	Error (%) $\frac{\lvert P_d - (P_d)_a \rvert}{(P_d)_a} \times 100$
0.2	2.5×10^{4}	4970	448.4	2.82	2.70	4
0.4	5×10^{4}	4959	459.4	2.89	2.91	< 1
4.0	5×10^{5}	4880	538.4	3.39	3.50	3
10.9	1.3×10^{6}	4839	579.4	3.65	3.72	2
40.0	5×10^{6}	4777	641.4	4.04	4.25	5
374	5×10^{7}	4635	783.4	4.93	5.19	5

1. $\Delta P = (P_{ave})_i - P_{wf}$

   $(P_{ave})_i$ = 5418.4 psi

2. $P_d = \frac{k_r h\, \Delta P}{(141.2)\, q_w \beta\mu} = \frac{(10)(3000)\ \Delta P}{(141.2)(15{,}000)(1.5)(1.5)} = 0.006295\ \Delta P$

3. From table 5, ref. 18.

TABLE 11. - Verification runs of horizontal well model

	Dimension (XxYxZ)	Well No.	Well type[1]	Wellblock coordinate
A.	15x15x1	1	V, WI, R	(8,1,1)
		2	V, WI, R	(8,15,1)
		3	H, OP, R	(7,7,1),(8,8,1),(9,9,1)
B.	15x15x1	1	V, WI, R	(8,1,1)
		2	V, WI, R	(8,15,1)
		3	H, OP, PI	(7,8,1),(8,8,1),(9,8,1)
C.	11x11x1	1	V, WI, R	(6,1,1)
		2	V, OP, PE	(6,11,1)
		3	H, WI, R	(1,5,1),(1,6,1),(1,7,1)
		4	H, OP, PI	(11,5,1),(11,6,1),(11,7,1)
D.	9x5x5	1	H, OP, PI	(4,3,3),(5,3,3),(6,3,3)

[1] V = vertical well.
H = horizontal well.
OP = oil production well.
WI = water injection well.
R = rate constraint.
PE = explicit pressure constraint.
PI = implicit pressure constraint.

TABLE 12 - Reservoir and well properties for pressure drawdown simulation of horizontal wells (Ozkan)

Porosity, %	22
Permeability, md	
Kx	19.67
Ky	19.67
Kz	4.92
Formation thickness, ft	50
Rock compressibility, psi^{-1}	6×10^{-5}
Oil formation volume factor	1.01
Oil viscosity, cp	1
Well radius, ft	0.33
Well length, ft	2000
Production rate, STB/day	2000
Production time, hours	500

TABLE 13. - Reservoir and well properties for pressure drawdown simulation of horizontal wells (Goode)

Porosity, %	10
Permeability, md	
Kx	100
Ky	100
Kz	100
Formation thickness, ft	220
Formation width, ft	2100
Well radius, ft	0.354
Well length, ft	500
Rock compressibility, psi^{-1}	3×10^{-5}
Oil formation volume factor, RB/STB	1.5
Oil viscosity, cp	1.5
Production rate, STB/day	3000
Production time, hours	1000

TABLE 14. - Reservoir and well properties for production simulation of slanted/horizontal/vertical wells

Porosity, %	22
Permeability, md	
Kx, Ky	1 to 100
Kz	0.1 to 100
Formation thickness, ft	50
Formation width/length, ft	1350
Oil formation volume factor, RB/STB	1.01
Oil viscosity, cp	1.0
Rock compressibility, psi^{-1}	6×10^{-5}
Formation pressure, psig	5000
Wellbore pressure, psig	4000
Well radius, ft	0.25
Production time, days	1830
Well length, vertical wells, ft	50
horizontal wells, ft	50 to 1350
slanted wells, ft	54 to 1351
Slant angles, slanted wells, degrees	22 to 88

TABLE 15. - Comparison of simulated production between horizontal and slanted wells of same well lengths from the plan view (Formation thickness = 50 ft)

Well length from plan view (ft)	Horizontal well length (ft)	Slanted well		Q_S/Q_H [1]
		Length (ft)	Angle (degree)	
50	50	70	45	1.152
100	100	112	63	1.015
200	200	206	76	0.991
350	350	354	82	0.983
750	750	752	86	0.948
1350	1350	1351	88	0.999

[1] Q_S = Cumulative oil production from slanted well after 5 years.
Q_H = Cumulative oil production from horizontal well after 5 years.

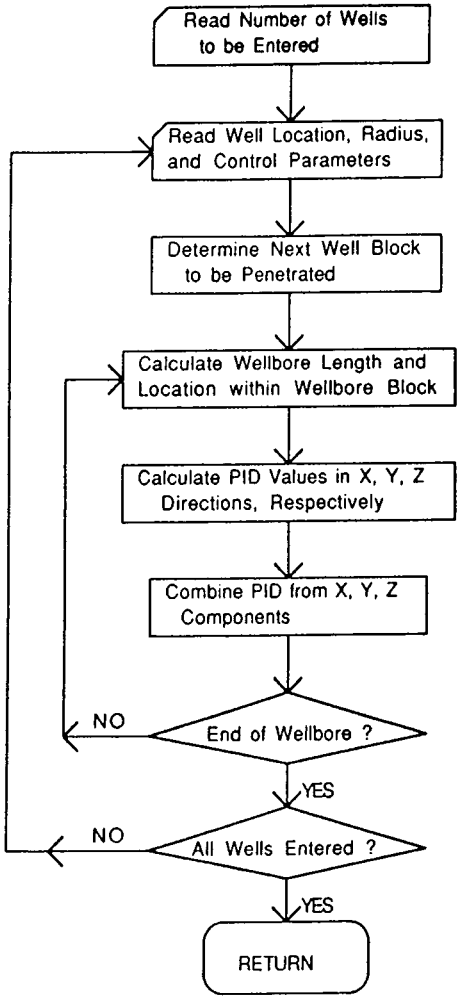

FIGURE 1. - Computer flow chart of slanted/ horizontal well model.

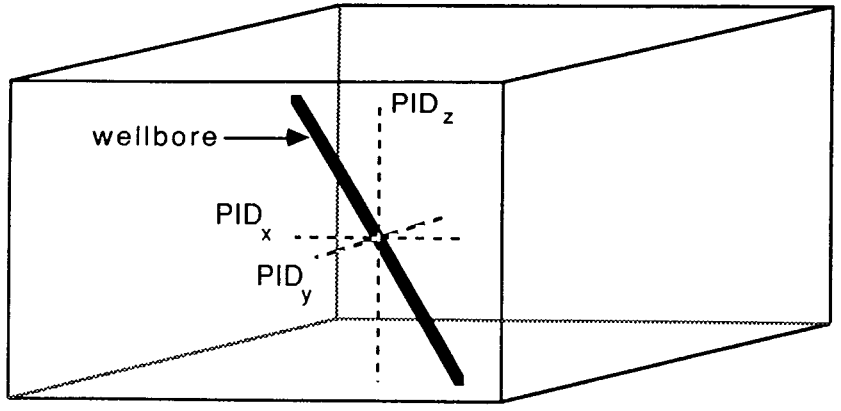

FIGURE 2. - Wellbore grid block and its three vector components of productivity index (PID).

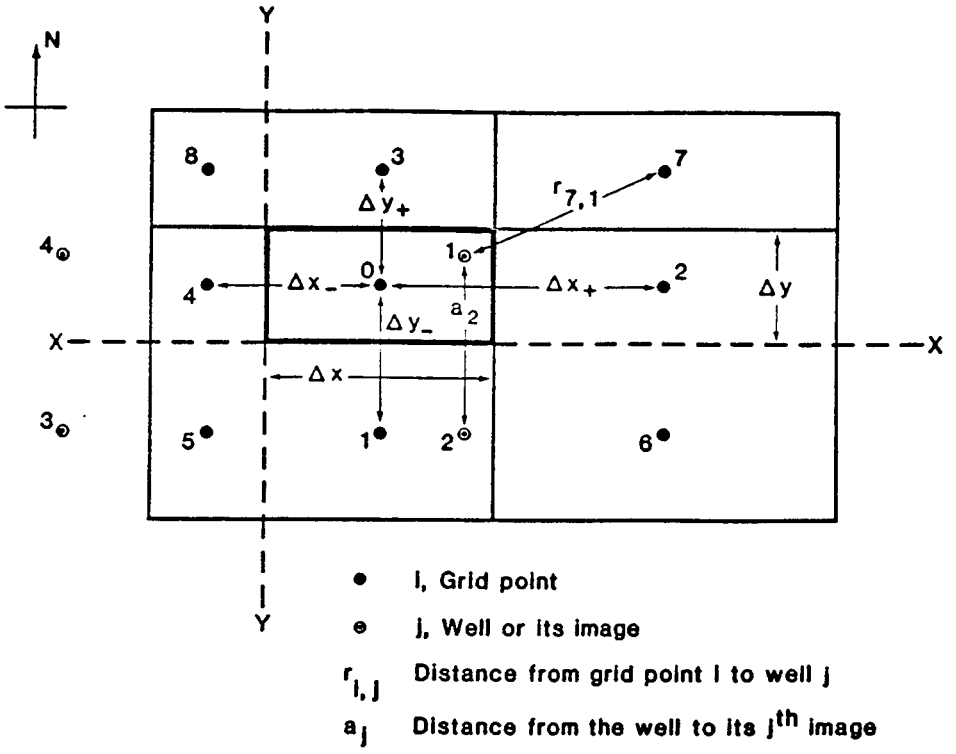

FIGURE 3. - Grid block 0 and its surrounding blocks (from Abou-Kassem and Aziz[30]).

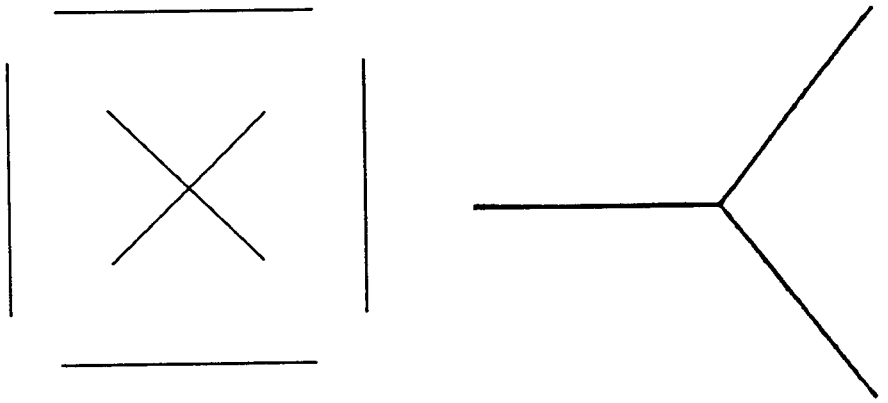

FIGURE 4. - Well pattern and drainhole geometry.

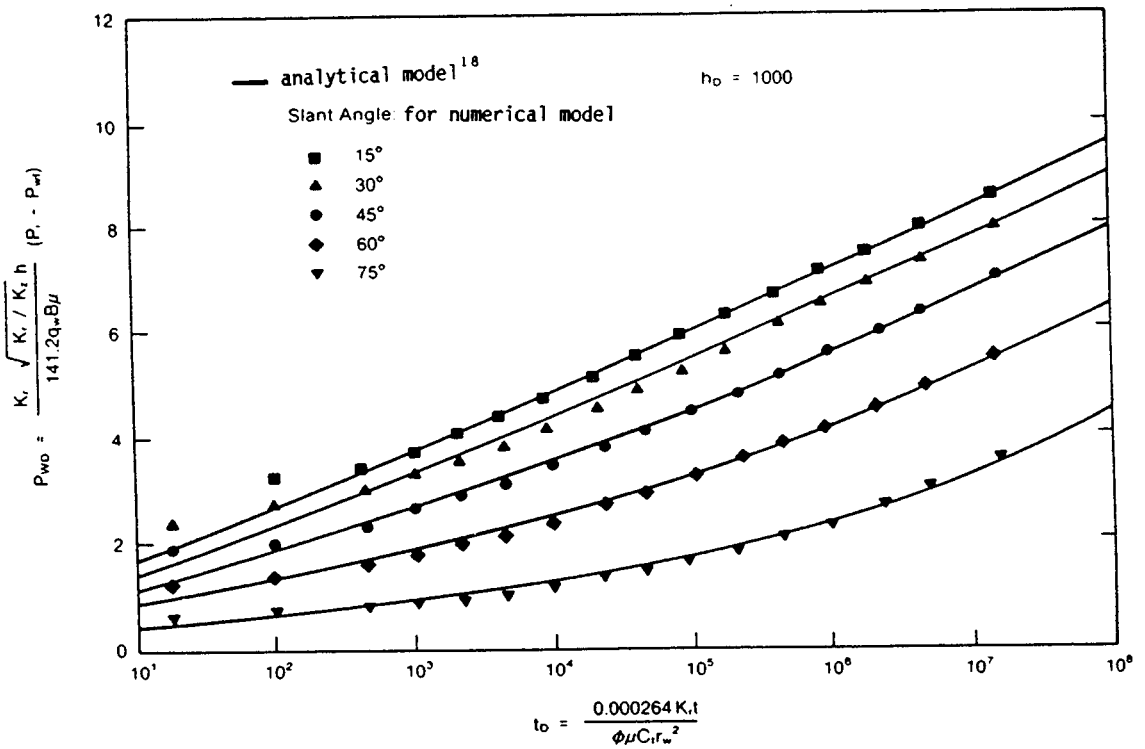

FIGURE 5. - Comparison between numerical and analytical models in pressure drawdown test of slanted well at various slant angles.

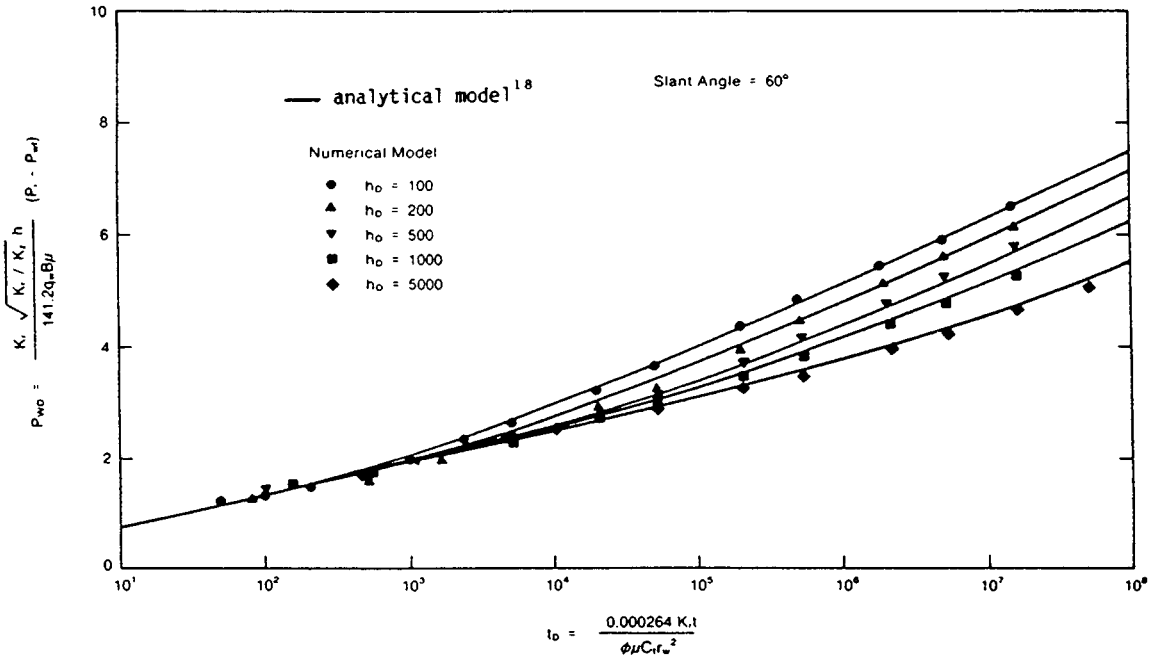

FIGURE 6. - Comparison between numerical and analytical models in pressure drawdown test of slanted well at various formation thickness.

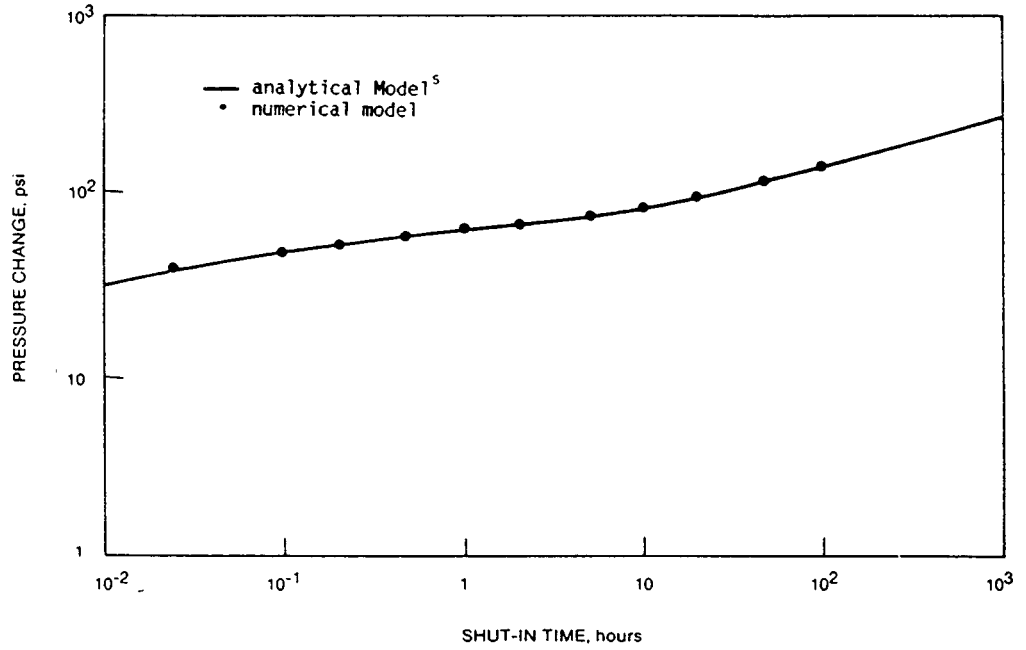

FIGURE 7. - Comparison between numerical and analytical models in pressure buildup test of horizontal well from an infinite field.

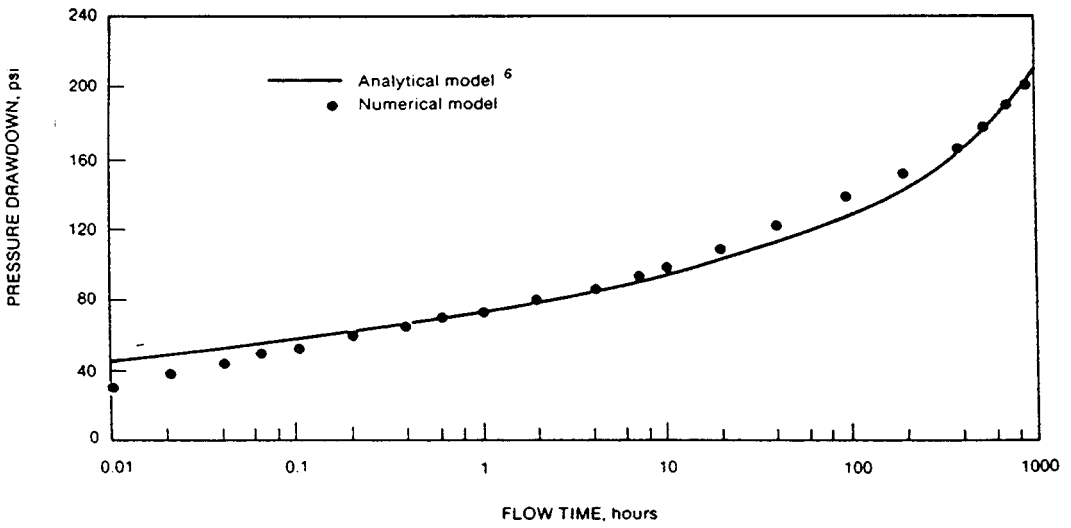

FIGURE 8. - Comparison between numerical and analytical models in pressure drawndown test of horizontal well from a semi-infinite field.

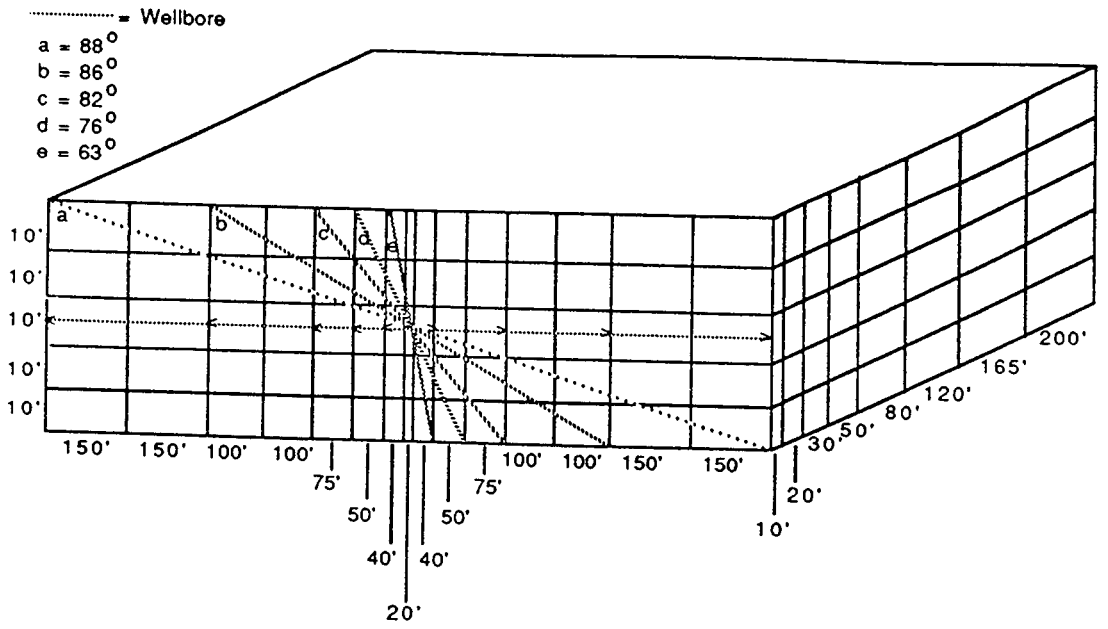

FIGURE 9. - Reservoir and wellbore grid for slanted, horizontal, and vertical well (slant angles are not drawn on scale).

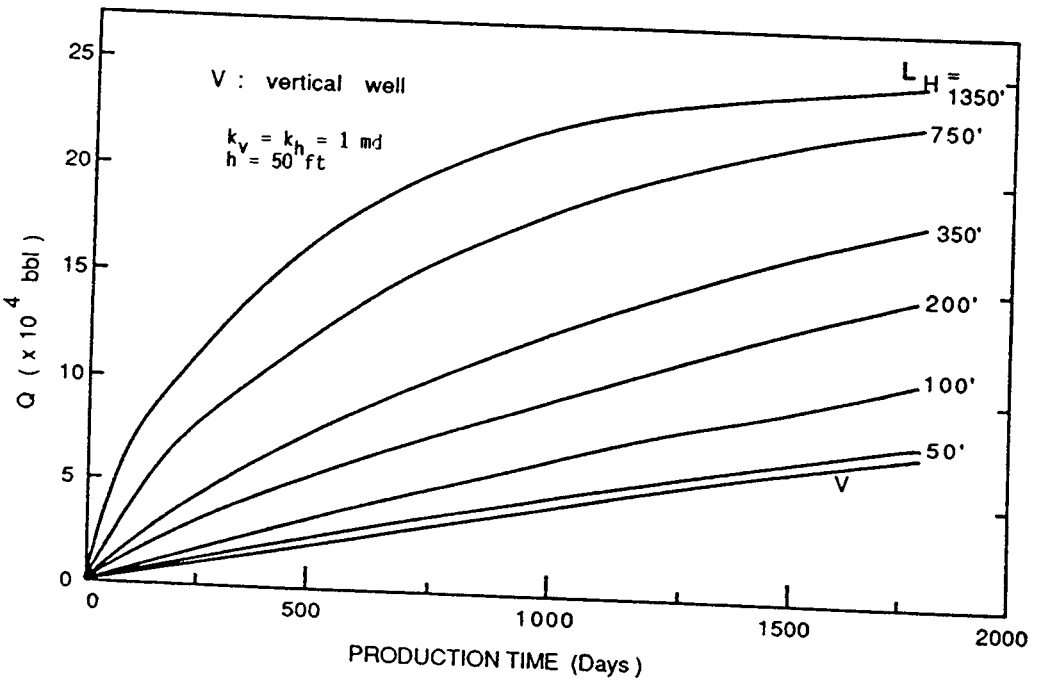

FIGURE 10.- Cumulative production from a vertical well and horizontal wells at various wellbore lengths. (L_H = length of horizontal well).

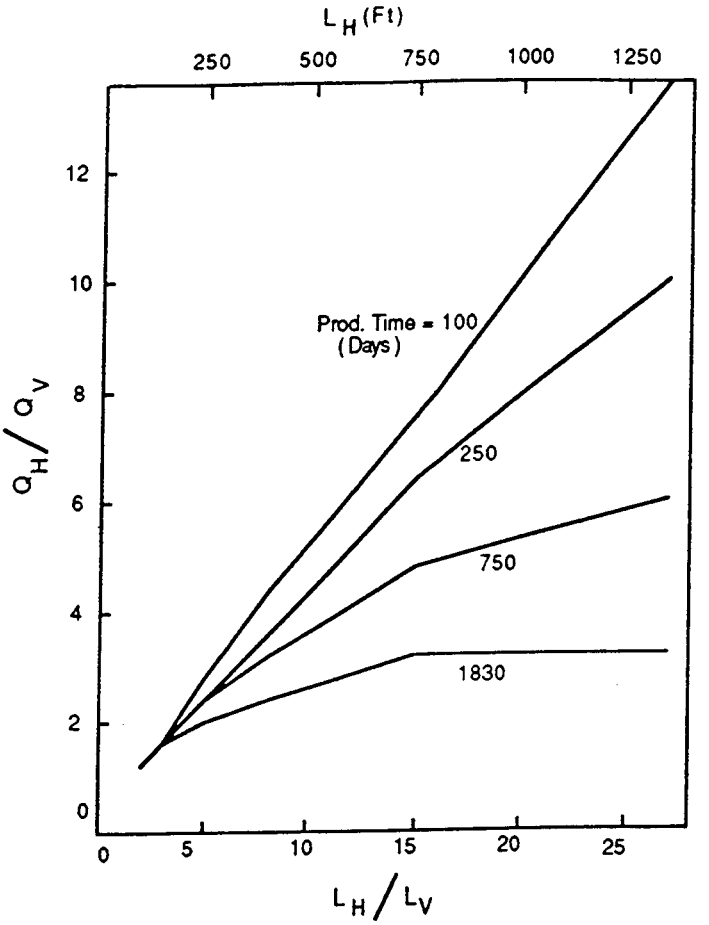

FIGURE 11. - Incremental cumulative production (Q) from incremental horizontal wellbore length after various production time (L = well length, H = horizontal well, V = vertical well).

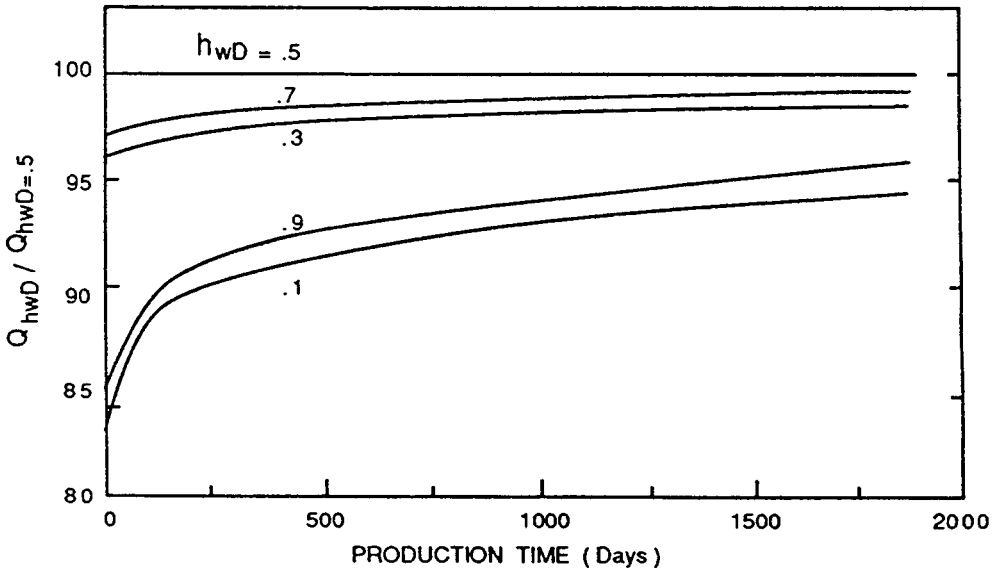

FIGURE 12. - Eccentricity effect on cumulative production (Q) from horizontal wells (h_{WD} = (Distance between wellbore and formation top)/ (pay thickness)).

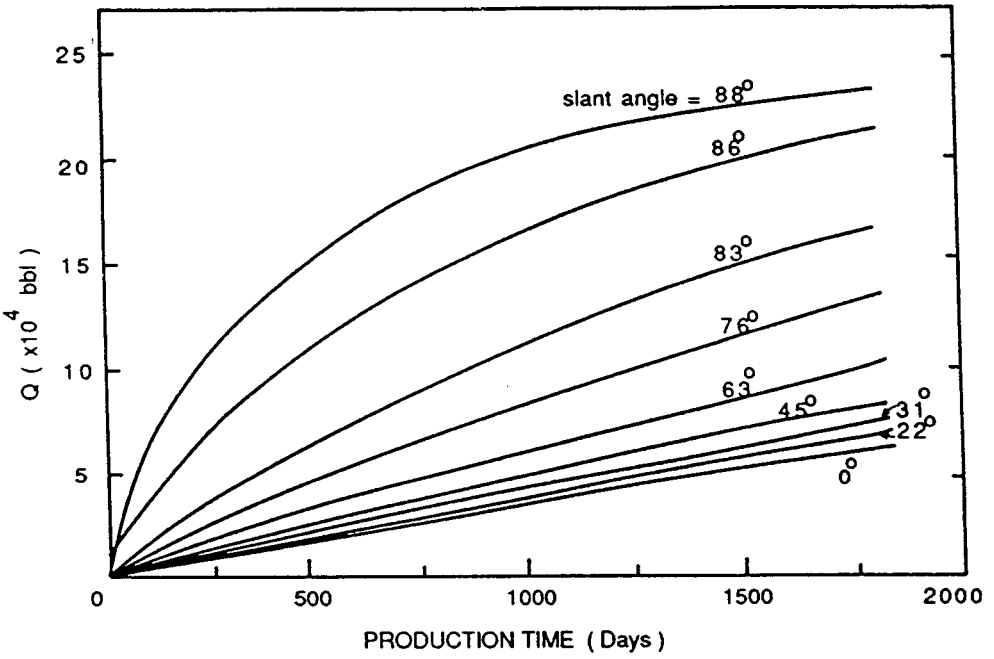

FIGURE 13. - Cumulative production from a vertical well and slanted wells at various slanted angles.

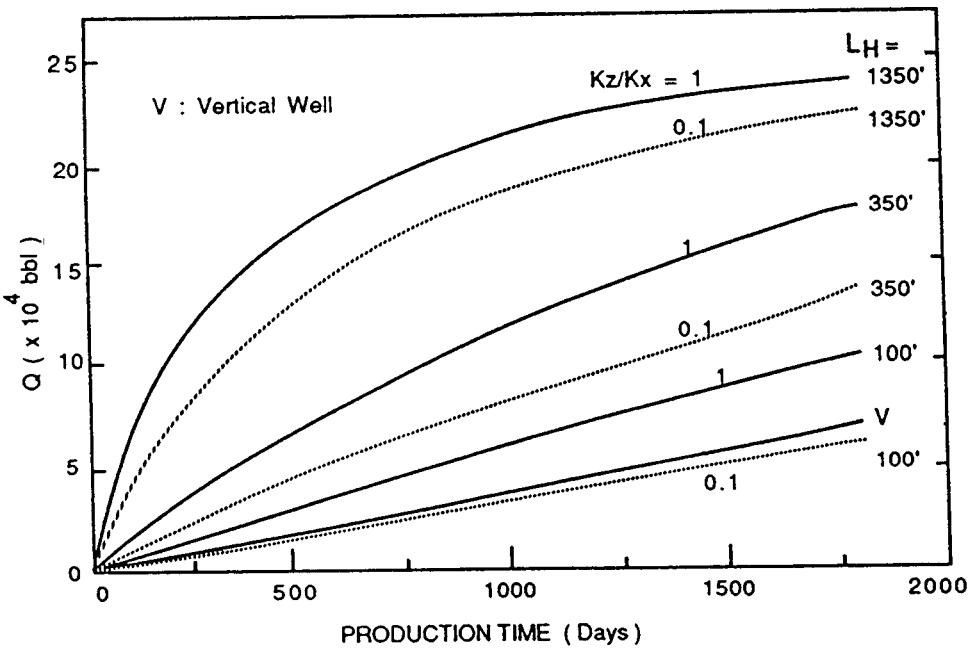

FIGURE 14. - Effect of vertical permeability on cumulative production (Q) of vertical and horizontal wells.

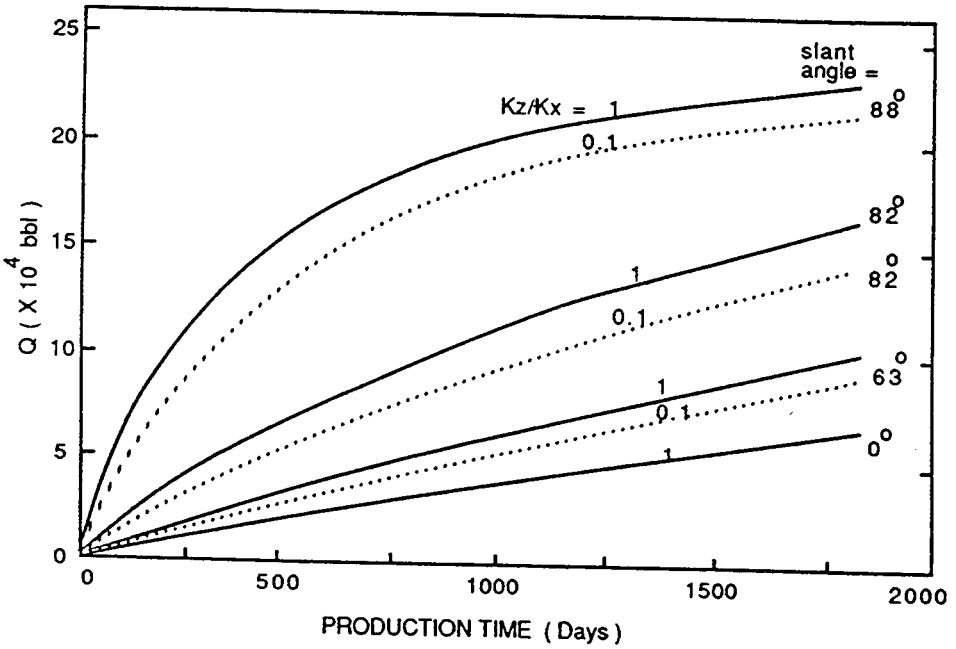

FIGURE 15. - Effect of vertical permeability on cumulative production (Q) of slanted wells.

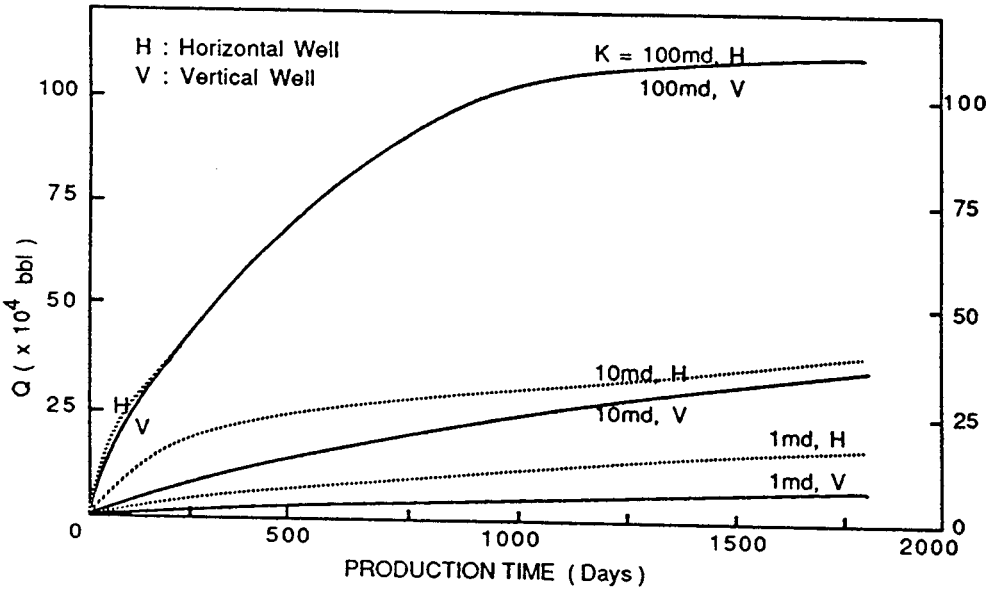

FIGURE 16. - Cumulative production from vertical and horizontal wells at various formation permeability.

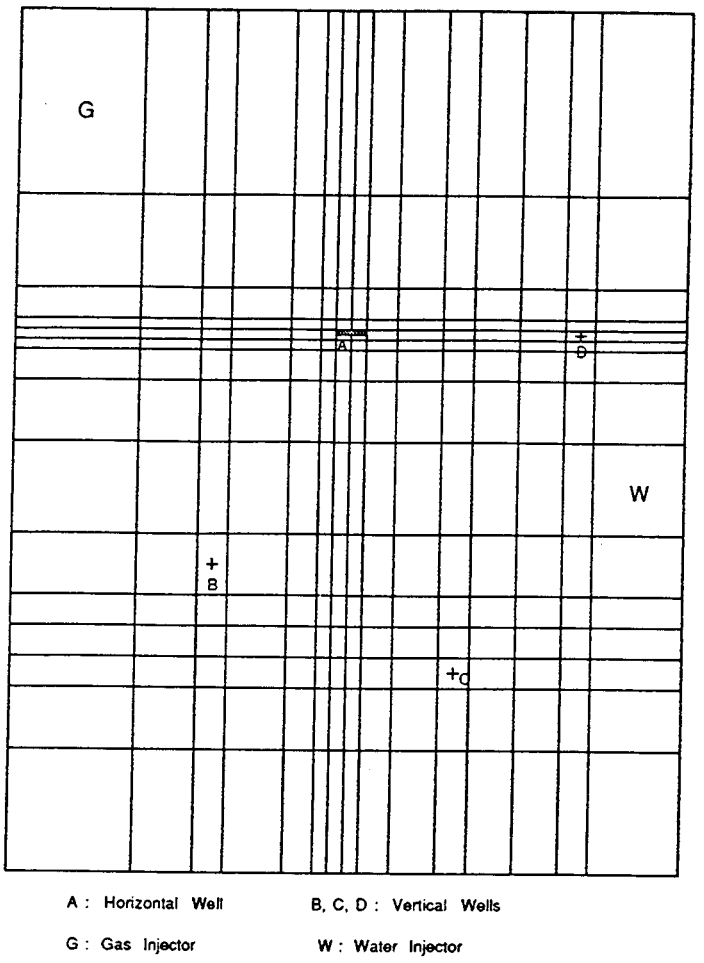

FIGURE 17. - Areal grid blocks and well locations in field simulation.

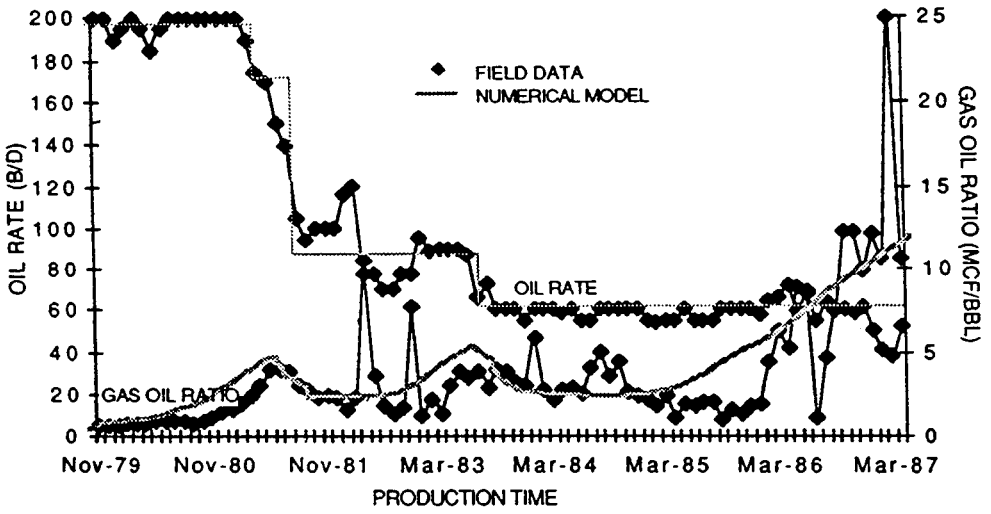

FIGURE 18. - Numerical history match of production from horizontal well.

☆U.S. GOVERNMENT PRINTING OFFICE: 1989-661-023/00042